

Synthesis of Functionalized Organoselenium Materials: Selenides and Diselenides Containing Cholesterol

Tiago E. Frizon,^[a,b] Jamal Rafique,^[a] Sumbal Saba,^[a] Ivan H. Bechtold,^[c] Hugo Gallardo,^[a] and Antonio L. Braga*^[a]

Keywords: Liquid crystals / Mesophases / Selenium / Steroids

A simple and efficient procedure for the synthesis of three new series of chalcogen liquid crystals, based on selenides and diselenides, containing cholesterol in their structure, is described. Thermal and liquid crystalline properties were investigated by POM, DSC, TGA and XRD scattering. Six of the nine molecules synthesized showed liquid crystal properties, with smectic mesomorphism. All the compounds pre-

sented good thermal stability. The smectic mesomorphism was confirmed through XRD analysis. The morphology of the surface of the films was investigated by using atomic force microscopy (AFM). All prepared diselenides showed good glutathione peroxidase like activity and one of the diselenides was 3.3 times more active than the standard Ebselen.

Introduction

In recent years, interest in organochalcogen compounds has been driven by their potential applications in modern organic synthesis of materials and in catalysis.^[1,2] Additionally, diorganodiselenides, the selenium counterpart of organic peroxides, play an important role in organochalcogen chemistry, because they are stable, easy to handle, and sufficiently reactive to produce electrophilic, nucleophilic, and radical species.^[3,4] The design of new organoselenium compounds, along with other developments, is attracting considerable attention, particularly because of their ability to mimic natural compounds with important biological properties, such as antioxidant, antitumor, antimicrobial, and antiviral activity.^[5–8] In addition, it has been shown that the presence of different chalcogen atoms in organic compounds can induce changes in their photophysical properties.^[9,10] Moreover, the photophysical properties allied with their liquid crystalline character mean that such materials are promising for optical device applications, such as emissive LC displays, polarized organic lasers, and anisotropic OLEDs. However, examples of the use of selenium compounds as liquid crystalline materials are rare.^[9] Organo

selenium derivatives have been studied in relation to the architecture of organic materials of technological interest; such compounds exhibit behavior that may be suitable for use in electroconductive polymers, organic semiconductors, and liquid crystals.^[9–15] Despite the potentially beneficial properties of applying diorganodiselenide compounds as constituent units in organic functionalized materials, to our knowledge, only the disulfide structures have been investigated.^[16,17]

In this context, the aim of this study was to associate the remarkable properties of selenium with the structure of cholesterol, to generate an important class of biological and synthetic materials in which the molecules are macroscopically arranged in a periodic helicoidal structure.^[18,19]

Cholesterol is a well-known natural product that appears as a building block in molecular associations. Its versatility comes from its unique structural features, which are not found in other compounds. Cholesterol is extensively incorporated in molecular systems for a number of reasons: (i) it is commercial availability; (ii) it has a rigid structure with eight chiral centers; and (iii) the structure can be easily derivatized.^[18–20] Derivatives of cholesterol are present in several unique aggregates, including liquid crystals, organic gels, and monolayers, making it a versatile building block in organic synthesis.^[21,22] The self-assembly of cholesterol-derived compounds into thermotropic liquid crystalline (LC) phases is well known. In fact, the first observation of LC phases was reported for cholesteryl benzoates and cholesteryl acetates.^[23] According to their chemical nature, cholesteric liquid crystals can be divided into: (a) steroidal, mainly cholesterol esters; (b) nonsteroidal, better known as chiral nematics; and (c) induced cholesteric systems, comprised of a nematic matrix and an optically active

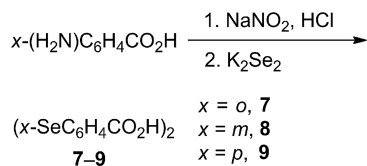
[a] Department of Chemistry LabSelen, Federal University of Santa Catarina (UFSC), 88040-900 Florianópolis, Brazil
E-mail: braga.antonio@ufsc.br
<http://ppgqmc.posgrad.ufsc.br/braga/>

[b] Department of Materials Science and Engineering, Universidade do Extremo Sul Catarinense, 88806-000 Criciúma, SC, Brazil

[c] Department of Physics, Federal University of Santa Catarina (UFSC), 88040-900 Florianópolis, Brazil

Supporting information for this article is available on the WWW under <http://dx.doi.org/10.1002/ejoc.201500124>.

matic amines (2-aminobenzoic acid, 3-aminobenzoic acid, and 4-aminobenzoic acid) into their respective diazonium salts, using NaNO_2 and HCl , which were added to a solution of K_2Se_2 (prepared using KOH and elemental selenium), resulting in diselenides **7**, **8**, and **9** with 51, 48, and 43% yield, respectively.



Scheme 3. Intermediate selenides **7–9**.

The synthesis of the nonsymmetrical selenides **10–12** and symmetrical diselenides **13–18** was carried out through the esterification of selenides **1–3** and diselenides **4–9** with the steroid cholesterol, employing a standard procedure that is widely used to activate carbonyl groups in a nucleophilic substitution, using *N,N*-dicyclohexylcarbodiimide (DCC)/4-(*N,N*-dimethylamino)pyridine (DMAP). The yields obtained in the synthesis of cholesterol derivatives **10–18** after

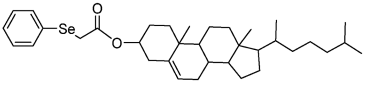
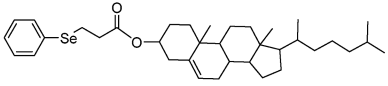
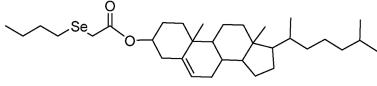
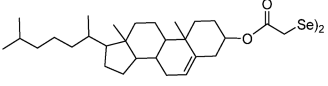
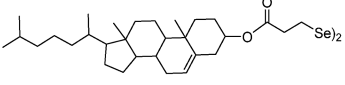
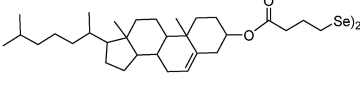
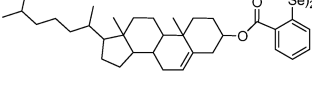
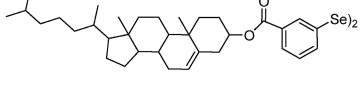
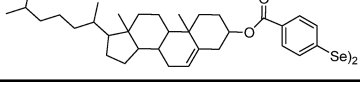
purification by column chromatography are shown in Figure 1.

Thermal and Mesomorphic Behavior

The mesomorphic properties of the final compounds were investigated by polarized optical microscopy (POM), differential scanning calorimetry (DSC), and X-ray diffraction (XRD) analysis. The thermal stability was verified by thermogravimetric analysis (TGA). The transition temperatures and enthalpy values (kJ mol^{-1}) of the compounds were collected from the second heating scan and are summarized in Table 1. According to the TGA traces, all compounds exhibited good thermal stability and their decomposition temperatures were between 203 and 330 °C.

Six of the nine molecules synthesized displayed liquid crystal properties. Compounds **12** and **15** exhibited a SmC^* mesophase, whereas compounds **16–18** showed a chiral enantiotropic smectic A (SmA^*) mesophase. Compound **14** displayed both SmC^* and SmA^* mesophases on heating, but only SmC^* on cooling. Compound **11** remained in a supercooled state until room temperature.

Table 1. Transition temperatures (°C) and associated enthalpy values (kJ mol^{-1} , in parentheses) for compounds **10–18**.

Compound ^[a]	Structures	Transitions ^[a]	Temp.(dec.) [°C] ^[b]
10		Cr 98.0 (26.4) I I 47.0 (14.6) Cr	203
11		Cr 47.1 (16.5) I	241
12		Cr 153.4 (17.4) SmC^* 160.7 (0.2) I I 157.7 (0.4) SmC^* 139.2 (18.0) Cr	233
13		Cr 160.7 (18.0) I I 141.1 (23.1) Cr	295
14		Cr 83.5(10.4) SmC^* 90.0 (2.2) SmA^* 113.8 (5.9) I I 112.5 (6.7) SmC^* 87.8 (3.1) Cr	305
15		Cr 136.7 (33.1) I I 124.1(7.4) SmC^* 48.8 (3.1) Cr	310
16		Cr 211.0 (26.4) SmA^* 225.0 (5.2) I I 213.0 (2.8) SmA^* 189.0 (33.5) Cr	321
17		Cr ₁ 113.0 (8.2) Cr ₂ 165.0 (2.7) SmA^* 198.0 (16.5) I I 179.0 (6.8) SmA^* 155.0 (20.1) Cr	313
18		Cr 127.9 (16.4) SmA^* 187.9 (5.1) I I 176.6 (3.8) SmA^* 88.0 (14.1) Cr	302

[a] DSC (10 °C min⁻¹). [b] TGA, onset of decomposition (10 °C min⁻¹).

For the symmetric alkyl diselenides **13–15**, a dependence of the melting points on the chain length was observed, as expected. It can be seen that as the internal chain length increases the melting points decrease and the clearing points increase, reducing the liquid crystalline range. Compound **13**, with only two internal spacer CH₂ groups, did not show liquid crystalline behavior, but by increasing the number of internal spacer CH₂ groups to four, the appearance of two mesophases for compound **14** (SmC* and SmA*) was observed. With a further increase in the internal chain length, the rigidity of the molecule decreased, leading to the appearance of only one mesophase SmC* for compound **15**. When the number of internal spacer CH₂ groups was more than four, the compounds can assume other conformations, although some of them are not appropriate, leading to the loss of mesomorphism.^[38]

Compounds **12**, **14**, and **15** presented similar schlieren texture of the mesophase SmC*. A representative texture presented by compound **14** at 90 °C is shown in Figure 2.

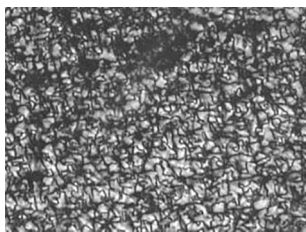


Figure 2. Schlieren texture of the mesophase SmC* observed on cooling the isotropic liquid at 90 °C, for diselenide **14**.

The DSC thermogram (Figure 3) for compound **12** indicated clearly the presence of two endothermic peaks, during heating cycles. On cooling, the DSC trace displays the same behavior as that seen during the heating cycle, presenting only one type of mesophase (SmC*). The DSC thermogram for compound **14** had three peaks during the heating cycle, representing mesophase transitions at 83 °C to a SmC*, 90 °C to an SmA* mesophase, and 114 °C to the isotropic liquid. During the cooling cycle, two peaks were observed and it was possible to note the presence of only the SmC* mesophase at between 112 and 87 °C.

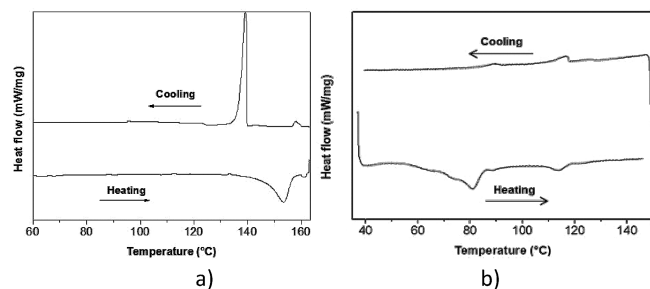


Figure 3. DSC traces of compounds **12** and **14** (respectively **a** and **b**) at a rate of 10 °C min⁻¹; 2nd heating and cooling runs are shown.

Compounds **16–18** have a higher structural rigidity than those of **12–14** cited above. This is a characteristic of great importance for obtaining mesomorphic compounds of SmA. Figure 4 shows the texture SmA* presented by com-

pound **17** at 189 °C. Similar textures were observed for compounds **16** and **18**.

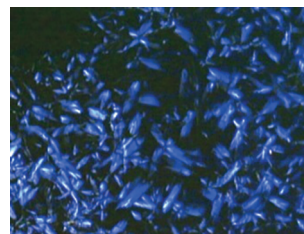


Figure 4. Batonnet texture of SmA* mesophase presented by diselenide **17** at 189 °C.

The DSC thermogram (Figure 5) for compound **18** indicated clearly the presence of two endothermic peaks during the heating cycles. On cooling, DSC analysis revealed an isotropic–SmA* transition at 176.6 °C and a SmA*–crystal transition at 88 °C.

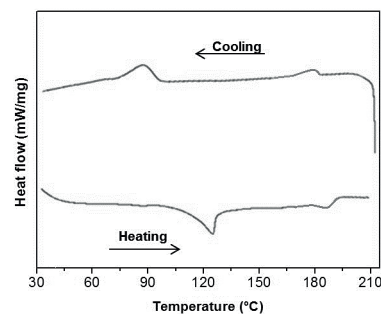


Figure 5. DSC traces of compound **18** for rates of 10 °C min⁻¹; 2nd heating and cooling runs are shown.

For the formation of the mesomorphism, one must consider the most stable conformation and structure of diselenide shown in the *trans* form. It is well known that molecules with dielement Y–Y (Y = S or Se) bonds are prone to exist in skewed conformations.^[39–41] The dihedral C–Y–Y–C angles for these compounds are much the same, with their mean angle falling somewhere between 80–90°. Consideration should be given to compound **16**, with a close-contact O...Se interaction, providing greater linearity and stability to the molecule, resulting in a higher clearing point. The temperature range of the mesomorphic behavior observed for compounds **16–18** was 27 to 90 °C.

X-ray Diffraction

XRD experiments were carried out on compounds **12** and **18** to investigate the smectic structure exhibited by the mesophases by following a procedure published elsewhere.^[42] All the recorded patterns contained a sharp peak in the low-angle region, arising from the reflection of the X-ray beam on the smectic layers, and corresponding higher-order peaks identified by the Miller indices (*hkl*). The interlayer spacing was obtained by applying Bragg's law to the first maximum (001). Figure 6 shows the pattern of compound **12** in the SmC* (153 °C), and the spectrum was very similar for compound **18**.

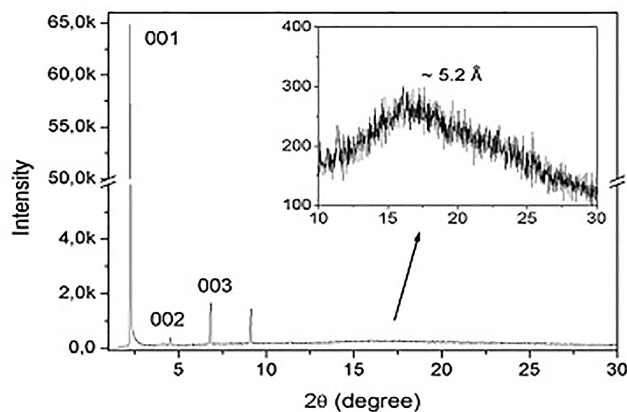


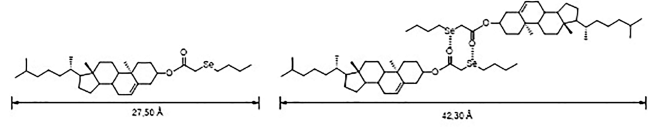
Figure 6. XRD pattern for compound **12** in the SmC* phase at 153 °C, with the Miller indices indicated. Inset shows the halo in the wide-angle region.

The smectic order was confirmed by considering the ratio between the value obtained for the interlayer spacing of the first maximum (d_{001}) and the values obtained for the secondary peaks (d_{00x} , with $x = 2$ and 3). It is well known that this ratio must obey the relation 1:2:3 in smectic phases (see all values of d_{001}/d_{00x} in Table 2). The inset of Figure 6 shows a diffuse halo in the high-angle region that is related to the short-range correlations between neighboring molecules within the smectic layers, corresponding to an average distance of 5.2 Å.

Table 2. X-ray diffraction data for the mesophases of compounds **12** and **18** on cooling. Schematic representation of the dimeric structure formed by selenide **12** in the SmC* layers.

Compound	Phase/ T [°C]	Length [Å]	(hkl)	d_{obs} [Å]	d_{001}/d_{00x}
12	SmC*/153	$l = 27.5$ $l_d = 42.3$	001	38.9	2.00
			002	19.4	3.03
			003	12.8	
18	SmA*/18	$l = 43.3$	001	41.8	2.00
			002	20.9	2.98
			003	14.0	

Selenide **12**



The molecular length (l) of each compound was estimated by using the ChemBio3D Ultra Software, version 11.0.1. The molecular length calculated for compound **12** was $l = 27.5$ Å. On comparing this length with the interlayer distance of $d_{001} = 38.9$ Å, a tendency toward the formation of antiparallel dimers can be noted, which is due to the well-known close-contact interaction between O and Se,^[43] as illustrated in Table 2. Comparing l_d with d_{001} reveals that the distance measured for the SmC* layers is 3.4 Å

lower, which is related to the inclination of the molecules and to the conformational disorder of the aliphatic chains. In the case of compound **18**, $l = 43.3$ Å, considering the most extended configuration.

In this case, a difference of only 1.5 Å is observed with respect to the interlayer distance (d_{001}), which can be considered to be associated with the conformational disorder of the aliphatic chains where, as in the SmA* phase, the molecules are oriented perpendicular to the molecular planes.

Morphological Aspects of Thin Films

Atomic force microscopy (AFM) was used to investigate the morphological aspects of spin-coated films of LC compounds **10–18**. The films obtained presented good homogeneity, as demonstrated by the AFM image of the film for compound **12** (Figure 7), with a mean surface roughness of around 7.5 nm. In addition, the films did not show the formation of crystallized domains.

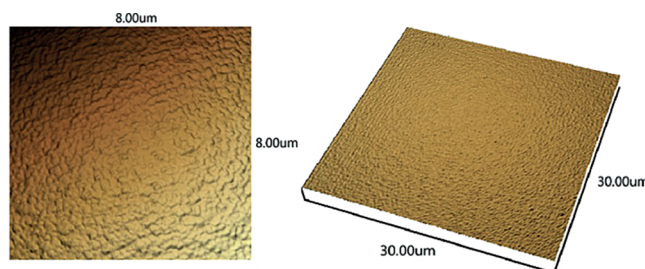


Figure 7. AFM images showing the surface morphology of solid films of compound **12**.

Glutathione Peroxidase-Like Activity

Glutathione peroxidase-like activity for all the diselenides **13–18**, was evaluated according to the Tomoda's method,^[44,45] using benzenethiol as a glutathione alternative. The reduction of H_2O_2 was monitored through the UV absorption increase at 305 nm, due to diphenyl disulfide formation. Ebselen was used as a standard in our studies (Table 3, entry 7). Most of the diselenides showed catalytic activity that was comparable to that of Ebselen, confirming that diselenide is a viable group to obtain GPx-mimetic agents. Notably, alkyl derivatives **14** and **15** provided the best results (entries 2 and 3). For example, compound **14** was 3.39 times more active than Ebselen, whereas **15** was

Table 3. GPx-like activity of diselenides **13–18**.

Entry	Catalyst	T_{50} [min]	Efficiency relative to Ebselen
1	13	138.34 (± 3.46)	1.09
2	14	44.76 (± 0.52)	3.39
3	15	76.10 (± 1.23)	1.99
4	16	126.81 (± 1.87)	1.19
5	17	108.70 (± 2.80)	1.39
6	18	117.05 (± 2.43)	1.30
7	Ebselen	152.17 (± 3.35)	1.00

1.99 times more active. Aromatic compounds **16–18** presented activity around 1.19–1.39 times higher than Ebselen. Further biological studies are in progress in our group.

Conclusions

We have synthesized three new series of chalcogen liquid crystals, based on selenides and diselenides, containing cholesterol in their structure. Six of the nine synthesized molecules showed liquid crystal properties. For the series of alkyl diselenides, a dependence of the melting points on the number of internal spacer CH₂ groups was observed. With an increase in the length of the internal chain, the compounds can assume other conformations, although some of them are not appropriate, leading to a loss of mesomorphism. Selenide **12** and alkyl diselenides **14** and **15** exhibited a SmC* mesophase, whereas aryl diselenides **16–18**, with a higher structural rigidity, showed a chiral enantiotropic smectic A (SmA*) mesophase. All synthesized compounds presented good thermal stability. The smectic mesomorphism was confirmed with the support of XRD analysis, from which we observed that compound **12** adopts a dimeric layered structure, as a result of the close intermolecular proximity, most likely from the nonbonding interaction between the O and Se atoms. Diselenides **13–18** all showed good catalytic activity that was comparable to that of Ebselen. Thus, we have described herein a new class of selenium compounds, containing cholesterol, with potential application as a new material with antioxidant properties. Further biological studies are in progress in our group.

Experimental Section

Materials and Characterization: All of the reagents were commercially available and were used without further purification. Organic solvents were of commercial grade and were dried by traditional methods. Column chromatography was performed by using column silica gel (230–400 mesh), and thin-layer chromatograph (TLC) was performed by using silica gel GF254 (0.25 mm), both purchased from Merck. ¹H and ¹³C NMR spectra were recorded with a Varian VXR spectrometer operating at 400 and 100.6 MHz, respectively. Melting points were determined with a Nikon Optishot 2 microscope equipped with a Mettler FP-82 Hot Stage. Elemental analysis was carried out with a Leco CHNS-932 instrument.

Thermal Analysis: Thermal transitions and enthalpies were determined from DSC measurements obtained using TA equipment with a Q2000 module or a Perkin–Elmer DSC-7 applying a heating/cooling rate of 10 °C min⁻¹ and a nitrogen flow of 50 mL min⁻¹. Thermal stability was investigated by TGA with a Shimadzu analyzer with a TGA-50 module, a heating rate of 10 °C min⁻¹ and nitrogen flow of 20 mL min⁻¹. Mesomorphic textures were determined with a Nikon Optishot 2 microscope equipped with a Mettler Toledo FP-82 Hot Stage and a Nikon Coolpix 995 digital camera.

X-ray Diffraction Analysis: The X-ray diffraction (XRD) experiments were performed with an X'Pert-PRO (PANalytical) diffractometer using the Cu-K_{α1} beam (λ = 1.5405 Å), with an applied power of 1.2 kVA. The samples were produced by following pre-

viously described procedures.^[42] The scans were realized in continuous mode from 2 to 30° (2θ angle) with the samples in the smectic phases by cooling from the isotropic state.

IR Spectroscopic Analysis: IR spectra were recorded with a Perkin–Elmer Spectrum 100 FTIR spectrometer with a resolution of 4 cm⁻¹ and in the 400–4000 cm⁻¹ wavenumber range (40 scans were co-added for the final spectrum). The compounds were sandwiched between two KBr windows and gently heated with a heating gun to better spread the sample. The measurements were taken at room temperature (25 °C).

Atomic Force Microscopy (AFM): AFM was used to investigate the morphological aspects of spin-coated films of compounds **10–18**. The AFM measurements were carried out with Shimadzu SPM-9700 equipment, with dynamic mode scanning.

Mass Spectrometry: The mass spectrometry (MS) system consisted of a hybrid triplequadrupole/linear ion trap mass spectrometer (Q Trap 3200, Applied Biosystems/MDS Sciex, Concord, Canada). Analyst version 1.5.1 was used for the LC/MS/MS system control and data analysis. The mass spectrometry was tuned in the negative and positive modes by infusion of a polypropylene glycol solution. The experiments were performed with a TurboIonSpray source (electrospray-ESI). High-resolution mass spectra (HR-MS) were recorded with a Bruker BioApex 70e FT-ICR (Bruker Daltonics, Billerica, USA) instrument in ESI mode.

Determination of GPx-Like Activity: The catalytic GPx model reaction (H₂O₂ + 2PhSH → 2H₂O + PhSSPh) was initiated by the addition of H₂O₂ (final concentration: 5 mM) to a solution of methanol (or ethanol when necessary), final volume: 1 mL, of thiophenol (PhSH) (final concentration 2 mM) containing the selenium catalyst (final concentration: 0.1 mM) at 25(±3) °C. The reduction of H₂O₂ was monitored by UV spectrophotometry, at 305 nm, through the formation of PhSSPh. The reaction was monitored for 150 s, at least three times under the same conditions. Activities of the compounds were compared with the activity of Ebselen as a positive control.

Acknowledgments

The authors are grateful to the Coordenação de Aperfeiçoamento de Pessoal de Nível Superior (CAPES), the Conselho Nacional de Desenvolvimento Científico e Tecnológico (CNPq/INCT), the Institutos Nacionais de Ciência e Tecnologia – Catálise (INCT-Catálise), the The World Academy of Sciences (TWAS) and the Fundação de Amparo à Pesquisa do Estado de São Paulo/Programa de Apoio a Núcleos de Excelência (FAPESC/PRONEX) for financial support. The Laboratório Central de Biologia Molecular Estrutural (CEBIME-UFSC) is thanked for the HRMS analysis.

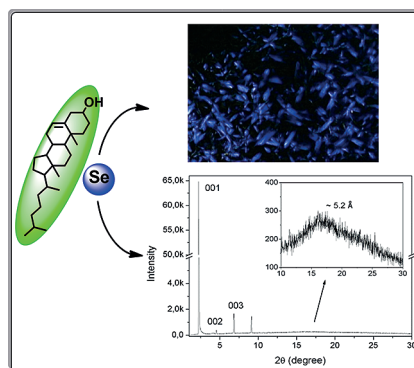
- [1] A. Seed, *Chem. Soc. Rev.* **2007**, *36*, 2046–2069.
- [2] D. M. Freudendahl, S. Santoro, A. Shahzad, C. Santi, T. Wirth, *Angew. Chem. Int. Ed.* **2009**, *48*, 8409–8411; *Angew. Chem.* **2009**, *121*, 8559.
- [3] H. Rheinboldt, *Method. Org. Chem. (Houben-Weyl)* **1955**, *9*, 949.
- [4] C. Paulniier, in: *Selenium Reagents and Intermediates in Organic Synthesis* vol. 5 (Ed.: J. E. Baldwin), Pergamon, Oxford, UK, **1986**.
- [5] C. W. Nogueira, G. Zeni, J. B. T. Rocha, *Chem. Rev.* **2004**, *104*, 6255–6286.
- [6] A. L. Braga, J. Rafique, *Synthesis of Biologically Relevant Small Molecules Containing Selenium, Part A, Antioxidant Compounds*, in: *The Chemistry of Organic Selenium and Tel-*

- lurium Compounds, Wiley, Chichester, UK, **2013**, vol. 4, p. 989–1052.
- [7] A. L. Braga, J. Rafique, *Synthesis of biologically relevant small molecules containing selenium*, Part B, *Anti-infective and anti-cancer Compounds*, in: *The Chemistry of Organic Selenium and Tellurium Compounds* (Ed.: Z. Rappoport), Wiley, Chichester, UK, **2013**, vol. 4, p. 1053–1117.
- [8] A. L. Braga, J. Rafique, *Synthesis of biologically relevant small molecules containing selenium*, Part C, *Miscellaneous biological activities*, in: *The Chemistry of Organic Selenium and Tellurium Compounds* (Ed.: Z. Rappoport), Wiley, Chichester, UK, **2013**, vol. 4, p. 1119–1174.
- [9] D. S. Rampon, F. S. Rodembusch, S. Fabiano, J. M. F. M. Schneider, I. H. Bechtold, P. F. B. Gonçalves, A. A. Merlo, P. H. Schneider, *J. Mater. Chem.* **2010**, *20*, 715–722.
- [10] a) J. Gu, Z.-Z. Qiong, Y. Ding, H.-L. Chen, Y.-W. Zhang, C.-H. Yan, *J. Am. Chem. Soc.* **2013**, *135*, 8363–8371; b) J. Rafique, S. Saba, A. R. Rosario, G. Zeni, A. L. Braga, *RSC Adv.* **2014**, *4*, 51648–51652.
- [11] T. Y. Ohulchanskyy, D. J. Donnelly, M. R. Detty, P. Prasad, *J. Phys. Chem. B* **2004**, *108*, 8668–8672.
- [12] M. R. Detty, P. B. Merkel, *J. Am. Chem. Soc.* **1990**, *112*, 3845–3855.
- [13] D. S. Rampon, F. S. Rodembusch, R. Lourega, P. F. B. Gonçalves, A. A. Merlo, P. H. Schneider, *J. Braz. Chem. Soc.* **2010**, *21*, 2100–2108.
- [14] A. Patra, Y. H. Wijsboom, G. Leitus, M. Bendikov, *Chem. Mater.* **2011**, *23*, 896–906.
- [15] G. Marin, A. L. Braga, A. S. Rosa, F. Z. Galetto, A. R. Burrow, H. Gallardo, M. W. Paixão, *Tetrahedron* **2009**, *65*, 4614–4618.
- [16] B. Du, B. Jin, P. Sun, *Org. Lett.* **2014**, *16*, 3032–3035.
- [17] M. H. Lee, Z. G. Yang, C. W. Lim, Y. H. Lee, D. B. Sun, C. H. Kang, J. S. Kim, *Chem. Rev.* **2013**, *113*, 5071–5109.
- [18] G. S. Chilaya, *Rev. Phys. Appl.* **1981**, *16*, 193–208.
- [19] G. S. Chilaya, L. N. Lisetski, *Mol. Cryst. Liq. Cryst.* **1986**, *140*, 243–286.
- [20] G. S. Chilaya, *Crystallogr. Rep.* **2000**, *45*, 871–886.
- [21] G. S. Chilaya, L. N. Lisetski, *Sov. Phys. Usp.* **1981**, *24*, 496.
- [22] *Handbook of Liquid Crystal Research* (Eds.: P. J. Collings, J. S. Patel), Oxford University Press, New York, **1997**.
- [23] O. Lehmann, *Z. Phys. Chem.* **1889**, *4*, 462–472.
- [24] T. E. Frizon, D. S. Rampon, H. Gallardo, A. A. Merlo, P. H. Schneider, O. E. D. Rodrigues, A. L. Braga, *Liq. Cryst.* **2012**, *39*, 769–777.
- [25] T. Frizon, A. L. Braga, J. Rafique, W. C. Elias, A. M. Signori, J. B. Domingos, *Disseleneto derivado do colesterol, processo de obtenção e uso de um disseleneto*, Brazil Pat., BR1020130180955; **2013**.
- [26] Z. Li, Y. Liu, T. Wang, H. Ma, *Mol. Cryst. Liq. Cryst.* **2011**, *534*, 50–56.
- [27] O. E. D. Rodrigues, D. Souza, L. C. Soares, L. Dornelles, R. A. Burrow, H. R. Appelt, C. F. Alves, D. Alves, A. L. Braga, *Tetrahedron Lett.* **2010**, *51*, 2237–2240.
- [28] M. O'Neill, S. M. Kelly, *Adv. Mater.* **2003**, *15*, 1135–1146.
- [29] H. Iino, J. Hanna, *Opto-Electron. Rev.* **2005**, *13*, 259.
- [30] Y. Shimizu, K. Oikawa, K. Nakayama, D. Guillon, *J. Mater. Chem.* **2007**, *17*, 4223–4229.
- [31] S. Torii, T. Inokuchi, G. Asanuma, N. Sayo, H. Tanaka, *Chem. Lett.* **1980**, *9*, 867–868.
- [32] Y. Feng, J. K. Coward, *J. Med. Chem.* **2006**, *49*, 770–788.
- [33] T. G. Back, Z. Moussa, *J. Am. Chem. Soc.* **2003**, *125*, 13455–13460.
- [34] D. L. J. Clive, H. Cheng, *Synth. Commun.* **2003**, *33*, 1951–1961.
- [35] A. Schoeller, *Ber. Dtsch. Chem. Ges.* **1919**, *52*, 1517–1518.
- [36] W. R. Gaythewaite, J. Kenyon, H. Phillips, *J. Chem. Soc.* **1928**, 2280–2287.
- [37] F. M. Ramos, H. S. Zamora, M. E. C. Aldrete, E. M. Camargo, Y. M. Flores, M. S. García, *Eur. J. Med. Chem.* **2008**, *43*, 1432–1437.
- [38] R. M. Srivastava, R. A. W. N. Filho, R. Schneider, A. A. Vieira, H. Gallardo, *Liq. Cryst.* **2008**, *35*, 737–742.
- [39] A. L. Fuller, L. A. Scott-Hayward, Y. Li, M. Bühl, A. M. Z. Slawin, J. D. Woollins, *J. Am. Chem. Soc.* **2010**, *132*, 5799–5802.
- [40] K. Helios, A. Pietraszko, W. Zierkiewicz, H. Wójtowicz, D. Michalska, *Polyhedron* **2011**, *30*, 2466–2472.
- [41] H. Gallardo, F. R. Bryk, A. A. Vieira, T. E. Frizon, G. Conte, B. S. Souza, J. Eccher, I. H. Bechtold, *Liq. Cryst.* **2009**, *36*, 839–845.
- [42] H. Gallardo, G. Conte, P. A. Tuzimoto, B. Behramand, F. Molin, J. Eccher, I. H. Bechtold, *Liq. Cryst.* **2012**, *39*, 1099–1111.
- [43] A. J. Mukerjee, S. S. Zade, H. B. Singh, R. B. Sunoj, *Chem. Rev.* **2010**, *110*, 4357–4416.
- [44] M. Iwaoka, S. Tomoda, *J. Am. Chem. Soc.* **1994**, *116*, 2557–2561.
- [45] A. L. Braga, E. E. Alberto, L. C. Soares, J. B. T. Rocha, J. H. Sudatia, D. H. Roos, *Org. Biomol. Chem.* **2009**, *7*, 43–45.

Received: January 26, 2015

Published Online: ■

A new series of selenide and diselenide liquid crystals containing cholesterol were synthesized and characterized. Most of the materials presented good thermal stability with SmC* and SmA* phases over a wide temperature range. The prepared diselenides also have potential biological applications, and they showed good antioxidant properties.



T. E. Frizon, J. Rafique, S. Saba,
I. H. Bechtold, H. Gallardo,
A. L. Braga* 1–8

Synthesis of Functionalized Organoselenium Materials: Selenides and Diselenides Containing Cholesterol



Keywords: Liquid crystals / Mesophases / Selenium / Steroids